Anal. Bioanal. Electrochem., Vol. 15, No. 8, 2023, 622-636
https://www.doi.org/10.22034/abec.2023.707323

Analytical &
Bioanalytical
Electrochemistry

2023 by CEE
www.abechem.com

Full Paper

From Mill Scale to Hematite: Processing and Electrophoresis Deposition Coating for Sustainable Secondary Battery Electrodes

Marcelinus Christwardana,[1,2,*] Zidane Kurniawan[3], and Deni Shidqi Khaerudini[4,*]

[1]*Department of Chemistry, Faculty of Science and Mathematics, Diponegoro University, Jl. Jacub Rais, Tembalang, Semarang, Indonesia 50275*
[2]*Master Program of Energy, School of Postgraduate Studies, Diponegoro University, Jl. Imam Bardjo SH, Pleburan, Semarang, Indonesia 50241*
[3]*Department of Chemical Engineering, Institut Teknologi Indonesia, Jl. Raya Puspiptek Serpong, South Tangerang, Indoensia 15314*
[4]*Research Center for Advanced Materials, National Research and Innovation Agency (BRIN), Kawasan Sains Teknologi BJ Habibie, Serpong, South Tangerang, Banten, 15314, Indonesia*

*Corresponding Author, Tel.: +6285647272844
E-Mails: marcelinus@lecturer.undip.ac.id (M. Christwardana); deni.shidqi.khaerudini@brin.go.id (D.S. Khaerudini)

Received: 7 April 2023 / Received in revised form: 3 August 2023 /
Accepted: 16 August 2023 / Published online: 31 August 2023

Abstract- Mill scale is a by-product of hot rolling steel generated in a rolling mill and has the potential to be transformed into hematite. Owing to hematite's many uses; mill scale has a high economic value and may be used as a battery anode. The impact of $CaCO_3$ pellet quantity and calcination time on hematite purity, as well as the effect of deposition duration and voltage on coating thickness. The calcination duration has a considerable effect on the purity of the resulting hematite, while the addition of $CaCO_3$ pellets lowered the purity by around 6%. Attaining the thickest hematite coating on an aluminium surface required a 40 V treatment and a deposition time of 30 minutes. Alternately arranged aluminium ions (Al^{3+}) and oxide ions (O^{2-}) form an ionic connection. Whereas aluminium ions on the surface of aluminium are positively charged, oxide ions are negatively charged in order to generate an electrostatic interaction. During the discharge phase, the voltage decreased from 1.02 to 0.70 V. This research contributes to the development of more efficient and effective manufacturing procedures for hematite and its battery anode applications.

Keywords- Charge-discharge; Cyclic voltammetry; Electrophoresis deposition; Electrostatic interaction; Ionic bonding

---

1. INTRODUCTION

Mill scale is a by-product of the hot rolling of steel produced in a rolling mill [1]. This mill scale is the crust that forms during the hot rolling or cold rolling stages of the steel-making process. During the hot rolling process, steel is heated to a temperature up to 900 °C; as a consequence of oxidation with the surrounding air, the surface of the steel experiences "scaling" (peeling); this peeling is also known as mill scale [2-5].

Using flame cleaning, water spray, and pickling, the mill scale is removed from the surface of the steel metal. For every ton of steel produced, 35 to 40 kg of mill scale can be created. In 2020, it is anticipated that Indonesia's steel manufacturing capacity will reach 13.67 million tons per year, thus producing about 341,750 to 390,571 tons at the plant scale [6]. The majority of mill scale debris is disposed of in open dumping landfills, which causes heavy metals to seep into the soil and groundwater, providing an environmental danger [7]. Thus, it is vital to further treat and use industrial scale waste in order to mitigate the negative environmental effects of factory scale and at the same time increase its added values.

To use factory-scale waste, help or characterization of the chemicals included on a factory scale is required. Iron oxides are abundant in mill scale, generally in the form of Wustite (FeO), Magnetite (Fe_3O_4), and Hematite (Fe_2O_3). The total Fe content of the mill scale exceeds 90 % [8]. In general, mill scale is only reused as a raw material for the production of metal (Fe) through a conventional reduction reaction. In this research, the mill scale will be oxidized using a calcination (roasting oxidation) procedure, causing the Wustite (FeO) and Magnetite (Fe3O4) present in the mill scale converted into only (pure) Hematite (Fe_2O_3) [9]. After mill scale has transformed into Hematite, the hue will become reddish. In this work, the inclusion of $CaCO_3$ aids in the heating process. Therefore, in this work, the $CaCO_3$ is employed as a heat storage media while heating the mill scale to produce a proper hematite phase.

The usage of lime ($CaCO_3$) was selected due to the abundance of lime supplies in Indonesia. The Indonesian archipelago has a vast quantity of lime resources, which are almost uniformly distributed. The actual quantity of limestone resources is unknown. Nevertheless, geological maps indicate that the potential for limestone in Indonesia is about 28,678 billion tons, of which 61,376 million tons are projected reserves and 28,616 billion tons are accessible reserves [10]. Limestone and its derivatives have been extensively used in several sectors as additive materials in the ferrous and non-ferrous metal smelting business, the glass industry, etc.

Hematite can be applied to a variety of high-end applications, including gas sensors used to detect LPG, nitrogen, and methane gas leaks, among others. Afterwards, it may be used as a raw material for pigments, battery anodes, etc. [11]. Due to the many applications of Hematite, mill scale has a significant economic value. Hematite (Fe_2O_3) is the most stable iron oxide due to its photochemical, catalytic, sensing, and magnetic capabilities. It has considerable use in photocatalytic components, red pigments, catalysts, magnetic materials, gas sensors, and anti-corrosion protective coatings [12,13].

Pulsed laser deposition (PLD), sputtering, metal organic chemical vapor deposition method (MOCVD), improved chemical vapor plasma deposition (PECVD), chemical vapor deposition, and spray pyrolysis have all been used to produce hematite (Fe_2O_3). This project uses the Electrophoretic Deposition (EPD) technique for the coating process. The EPD offers more benefits than earlier approaches, including a low cost, simple procedure, easy-to-control layer thickness, microstructural uniformity, and the ability to deposit on complicated and widely shaped substrates [14]. Organic solvents such as acetylacetone, acetone, and ethanol are used in the majority of investigations in the EPD method for producing ceramic coatings. Organic solutions usually have a lower dielectric constant than liquid solutions, which restricts the charge on the particles [15]. Therefore, if the EPD is conducted by the organic solutions, a stronger field strength is required. For the production of thick or thin ceramics, the employed liquid suspensions of EPD gain increasing interest due to their cheap cost, high efficiency, and environmental friendliness [16]. Thus, EPD is an effective approach for superimposing Hematite (Fe_2O_3) for battery electrode synthesis.

Hematite, an abundant and environmentally friendly iron oxide material, holds promise for utilization as a battery electrode using the EPD method. EPD offers a simple and cost-effective technique for depositing thin films of hematite onto conductive substrates, enabling its integration into battery electrodes [17]. It allows for efficient and controlled deposition of hematite particles by applying an electric field. EPD can be performed on various conductive substrates, making it versatile for integrating hematite into battery electrodes. Hematite's high theoretical capacity and suitable redox potential make it an attractive candidate for energy storage applications [18]. However, challenges such as low electrical conductivity and poor lithium-ion diffusion in hematite films need to be addressed [19]. Further research on optimizing the EPD process and hematite film properties could unlock the potential of hematite as a battery electrode material for sustainable energy storage.

In this study, the impact of varying amounts of $CaCO_3$ pellets and calcination time on the purity of hematite was investigated, along with the influence of deposition time and voltage on the thickness of the coating, and subsequently, its performance as a lithium battery cell was examined. The experimental techniques of cyclic voltammetry and charge-discharge analysis were employed to further investigate the characteristics of the coated hematite samples in relation to their battery performance.

2. EXPERIMENTAL SECTION

2.1. Preparation of Raw Materials for Mill Scale Calcination

Mill Scale from an Indonesian steel mill, crushed to a fine powder and sieved through a #300-mesh screen. As a pre-treatment, it is then heated at 200 °C for one hour to remove dirt and oil. Manufacture of pelletized limestone powder by crushing 0.8 grams of powder using a hydraulic lab press. Two minutes should be spent for pressing at 500 MPa to shape a 1 cm pellet diameter.

2.2. Mill Scale Oxidation Process

This procedure is designed to convert mill scale into Hematite. First, 10 pcs of $CaCO_3$ pellets were put at the bottom of the crucible, followed by 48 grams of mill scale powder and 10 pcs of $CaCO_3$ on the top pellets. Thus, the crucible formed a sandwiched layer of pellets-mill scale-pellets. Thereafter, the 30 pcs of $CaCO_3$ pellets were placed in the crucible in a similar manner. The crucible is then positioned in the centre of the tubular furnace, which is covered with a glass tube. During the calcination (heating) process, oxygen from the surrounding air is drawn into the tubular furnace by a blower attached to one side of the glass tube. The calcination procedure was performed at 900 °C and held for 2 hours. The same treatment was also performed at 900°C and held for 4 hours. The calcination procedure was conducted at a heating rate of 5°C per minute. As a consequence of the calcination process, the mill scale will transform into hematite and undergo agglomeration, necessitating four hours of ball milling to reduce the hematite to a powder. The weight ratio of mill scale powder to balls is 1:10 wt.%, with the weight ratio of ball size of big, medium, and small is 40:20:40.

2.3. Suspension solution, Electrode Manufacturing, and Electrophoretic Deposition Process

The 0.01 g of iodine was dissolved in 20 mL of acetylacetone solvent. The 1 g of hematite is weighed and dissolved in 15 mL of acetylacetone to create the second solution. On a hot plate, the two solutions were combined and stirred together. The SS316L stainless steel plate was sliced into 3x4 cm, then the SS316L plate was entirely wrapped in aluminium foil, and the plate's mass was then measured as the starting anode mass. After placing the electrodes in the suspension solution, the power supply applied voltages of 20, 40, and 60 V for 10, 20, and 30 minutes.

2.4. Battery Assembling Method

Hematite is deposited on an aluminium foil surface layer in the form of a circular to be tested as a Li-ion battery anode in a half-cell mode. The battery assembly is performed in the gloves box. The positive case, cathode, separator, anode, spacer, spring, and negative case are merged into a button cell testing of the Li-ion battery. The battery then assessed its cyclic voltammetry (CV) profile using a scan window of 0 to 2.90 V *vs.* Ag/AgCl, as well as its charge-discharge (CD) analysis.

3. RESULTS AND DISCUSSION

3.1. Effect of $CaCO_3$ Pellet Amount and Calcination Time on Hematite Purity Percentage

Table 1 displays the impact of varying the quantity of $CaCO_3$ pellets and calcination time on the hematite purity concentration value. From the graph, it can be seen that at the same number of pellets and different calcination times, the longer the calcination time, the greater the hematite purity, whereas at the same calcination time and different numbers of $CaCO_3$ pellets, the greater the number of pellets does not increase the hematite purity. A high number of pellets does not raise the quality of the hematite; on the contrary, the greater the number of pellets utilized, the lower the purity of the resulting hematite. This is owing to the fact that the greater the quantity of $CaCO_3$ pellets utilized, the smaller the air cavity going to the mill scale. As a result, the mill scale cannot respond to oxidation efficiently due to a lack of oxygen input from the outside. The mill scale in the centre of the layer does not get enough oxygen due to the vast quantity of pellets above it. The calcination period has a significant impact on the purity of the resultant hematite, since the longer the calcination time, the more uniformly the oxidation reaction will be dispersed to all areas of the mill scale powder [20]. However, it shows that the number of $CaCO_3$ pellets affects the purity level of the hematite phase formed. Indeed, retention time has a substantial impact as well on the hematite purity phase formed.

The $CaCO_3$ pellets are employed as a reducing agent in this process to transform non-hematite iron oxide into hematite. The following chemical reactions occur during this process:

$$FeO + CaCO_3 \rightarrow FeO.CaO + CO_2 \qquad (1)$$

$$Fe_3O_4 + 2CaCO_3 \rightarrow 2FeO.CaO + 2CO_2 \qquad (2)$$

The $CaCO_3$ pellets combine with non-hematite iron oxides (FeO and Fe_3O_4) to generate FeO, as shown by the above reaction. The CaO subsequently interacts with other iron oxides to generate pure hematite (Fe_2O_3). This process produces CO_2, which is discharged into the atmosphere. The amount of $CaCO_3$ pellets used in the mill scale refining process might affect the purity of the hematite produced. If the requisite quantity of $CaCO_3$ pellets is not met, not all of the non-hematite iron oxide will be transformed into hematite, resulting in impure hematite. However, if an excessive amount of $CaCO_3$ pellets is used, a large amount of CO_2 and FeO.CaO by-products will be produced, which might impair the quality of the resultant hematite. Consequently, the ideal quantity of $CaCO_3$ pellets must be used to guarantee that the reaction is successful and that the resultant hematite is very pure. In addition, other variables, such as temperature, time, and chemical concentrations, may influence the purity of the resultant hematite and must be considered concurrently in order to achieve an ideal output [21].

Table 1. Weight and percentage of hematite produced from various numbers of $CaCO_3$ pellets and time

Run	No. of Pellets	Time (h)	Weight of Mill Scale (g)	Weight of Magnetite (g)	Weight of Hematite (g)	Hematite Percentage (%)
1	20	2	44.894	4.184	40.71	90.68
2	20	4	34.219	0.044	34.18	99.87
3	30	2	31.930	5.364	26.57	83.30
4	30	4	47.585	3.058	44.53	93.57

3.2. Effect of Voltage and Deposition Time on Hematite Purity Percentage

The influence of deposition duration and voltage on coating thickness is shown in Table 2. From Table 2, when the deposition time and voltage input are increased, the resultant coating thickness will grow, however, there is a saturation threshold of the coating thickness beyond where the thickness will drop (spallation). From Figure 1, the thickest layer should be achieved when a voltage condition at 40 V treatment and a deposition duration of 30 minutes. This suggests that the voltage treatment and deposition duration have an optimum and selective condition on the particle size and thickness of the resulting layer.

Table 2. Weight of deposited hematite on the surface of the electrode from various voltage and deposition time

Run	Voltage (V)	Deposition Time (min)	Initial Weight of Electrode (g)	Final Weight of Electrode (g)	Weight of Deposited Hematite (g)
1	20	10	0.800	0.840	0.040
2	20	20	0.790	0.833	0.043
3	20	30	0.797	0.839	0.042
4	40	10	0.810	0.891	0.081
5	40	20	0.815	0.928	0.113
6	40	30	0.779	1.077	0.298
7	60	10	0.811	0.832	0.021
8	60	20	0.804	0.854	0.049
9	60	30	0.781	0.872	0.091

In accordance with Faraday's law, the relationship between voltage and layer thickness is such that the amount of substance deposited on the electrode after the electrophoretic deposition process is directly proportional to the electric charge through the electrolyte solution and proportional to the molecular weight of the substance [22]. In this instance, the voltage supplied to the electrodes might influence the quantity of electric charge in the electrolyte solution and, subsequently, the amount of material deposited. If the voltage or voltage delivered to the electrodes is raised, the quantity of electric charge that flows through the electrolyte solution will also rise [23]. Hence, the quantity of material deposited on the electrode's surface will rise, resulting in a thicker layer. In contrast, if the applied voltage or voltage to the electrode is decreased, the quantity of material deposited will decrease, resulting in a thinner layer (Figure 2). In addition to voltage, additional parameters such as deposition duration, temperature of the electrolyte solution, and concentration of the electrolyte solution may influence the thickness of the layer created during the electrodeposition process [24]. Thus, in order to maximize the required metal layer thickness, all parameters must be considered concurrently [25,26].

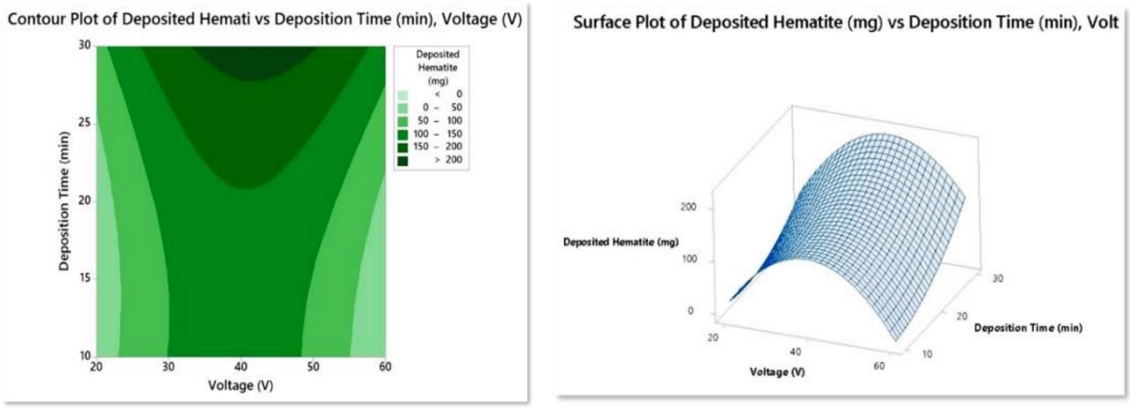

(a) (b)

Figure 1. a) contour and b) surface plot of deposition time and voltage effect on deposited hematite

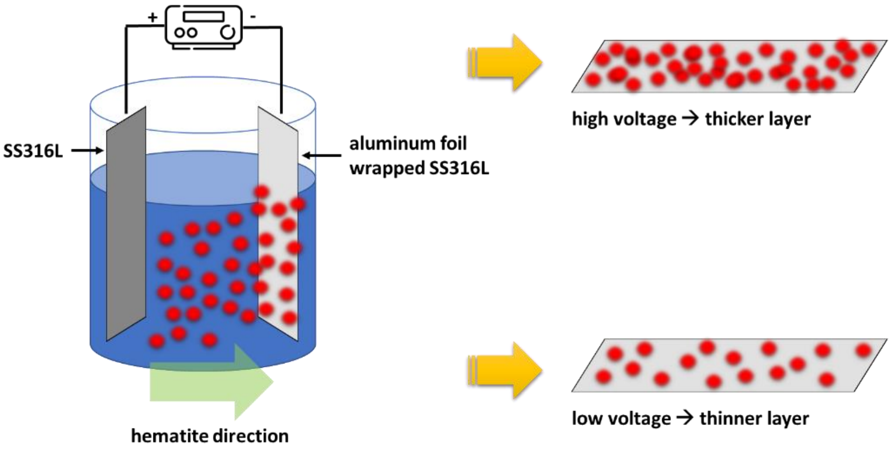

Figure 2. Illustration the relationship between voltage and layer thickness during EPD process

3.3. Morphology of hematite deposited on the aluminium surface

Figure 3a is an uncoated current collector made of aluminium. Because there is no additional layer concealing or altering the surface's appearance, the aluminium’s surface may appear clean and smooth upon morphological investigation. The surface of the aluminium will exhibit the metallic structure typically observed in purified metals, such as crystalline structures. Aluminium current collectors in Figure 3b and 3c have been coated with hematite from mill scale and oxalate, respectively. Hematite is a reddish-coloured iron oxide mineral with strong magnetic properties. The morphology of these two samples suggests that a layer of hematite covers the surface of the aluminium. This magnetite layer can make the aluminium's surface appear rougher and more structured. Due to their comparable hematite layers, morphological analysis reveals little difference between the two. The magnification of the surface of each current collector can be seen in Figure 3d - 3f.

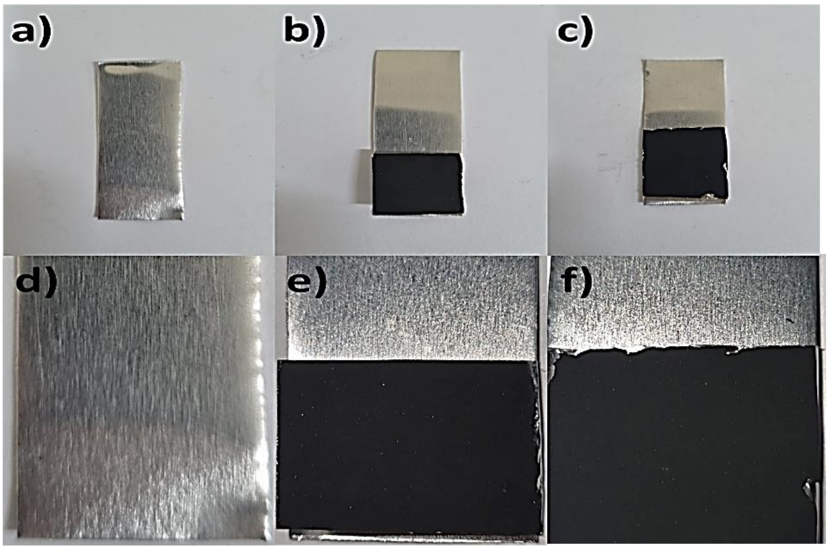

Figure 3. Photograph of a) bare aluminium current collector, b) hematite from mill scale - coated aluminium current collector, and c) hematite from oxalate-coated aluminium current collector. While d) – f) is their magnification

3.4. Interaction of hematite and aluminium during electrodeposition process

In the process of electrodeposition, hematite and aluminium form an ionic bonding by interactions between ions in the hematite layer and the oxidized aluminium surface, as shown in Figure 4. Hematite (Fe_2O_3) contains an alternating arrangement of iron (III) ions and oxide (O^{2-}) ions inside its crystal structure [27]. Iron (III) ions and oxide ions may combine with electrolyte ions and generate complex compounds in electrolyte solutions. Aluminium ions (Al^{3+}) and oxide ions (O^{2-}) are alternately organized in a crystal lattice on the oxidized aluminium surface, which likewise has a crystal structure [28]. Aluminium ions on the surface of aluminium will be positively charged, while oxide ions would be negatively charged [29,30]. Consequently, an attractive attraction exists between the oxide ions in the hematite layer and the aluminium ions on the surface of the oxidized aluminium. This contact may generate ionic connections between the ions in the hematite layer and the aluminium surface that has been oxidized. When the ions in the hematite layer attract aluminium ions on the oxidized aluminium surface towards the hematite surface, ionic connections are formed.

Since it includes an exchange of electrons between the ions, this ionic connection is very strong and difficult to break [31]. This process is thought may occur concurrently under electrodeposition circumstances when the electrolyte solution and the oxidized aluminium surface are utilized as the electrode media.

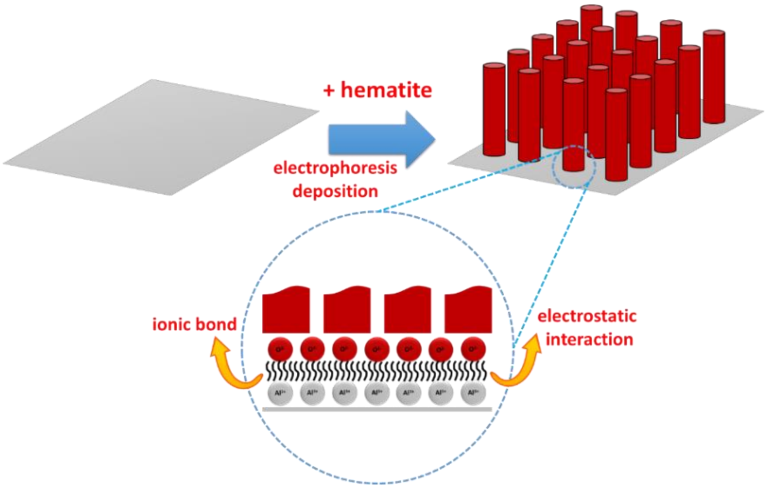

Figure 4. Bonding and interaction between aluminium and hematite after electrophoretic deposition process

3.5. Performance of battery which applies hematite anode from mill scale and oxalate

The GCD curves of a battery with a hematite anode from a mill scale are depicted in Figure 5a. Charge capacity ranges between 0.316 and 0.386 mAh, while discharge capacity ranges between 0.231 and 0.255 mAh. Comparatively, Figure 5b depicts the GCD curves of a battery with a hematite anode made from oxalate. The maximum charge capacity of the battery is between 0.763 and 0.812 mAh, while the maximum discharge capacity is between 0.625 and 0.636 mAh. On the basis of charge-discharge capacity data for batteries with hematite anodes derived from mill scale and oxalate, it is evident that batteries with hematite anodes derived from oxalate perform better than those derived from mill scale. This performance difference can be attributed to physical and chemical distinctions between the two hematite anode sources. The crystal structure and homogeneity of hematite derived from oxalate may be superior, allowing for more efficient charge transfer during the charge-discharge process [32]. In contrast, hematite from mill scale may contain flaws or impurities that reduce the battery's overall performance.

Figure 5c is a battery charge-discharge curve for three cycles per unit of time using hematite from a mill scale. According to the graph, each charge cycle takes roughly 230 minutes and each discharge cycle takes roughly 135 minutes. Figure 5d depicts the charge-discharge curve of an oxalate-based hematite battery. Each cycle requires a charging time of approximately 490 minutes and a discharge time of approximately 390 minutes. According to charge-discharge curve data from batteries with hematite anodes from mill scale and oxalate, hematite from mill scale batteries have a shorter charge and discharge time than hematite from oxalate batteries. Several factors, including the electrochemical properties of the two varieties of hematite anodes and the efficacy of the electrochemical reactions that occur during the charge-discharge process, can affect the difference in charge and discharge times. Hematite derived from mill scale may exhibit a more rapid and efficient reaction, resulting in reduced charge and discharge times. In contrast, hematite derived from oxalate may endure a more complex electrochemical reaction, requiring more time to achieve the same charge-discharge capacity [33]. This analysis demonstrates that the material properties of the hematite anode can impact the charge-discharge cycle time and the battery's overall performance.

The battery capacity using hematite from mill scale is depicted in Figure 5e. In the third charging cycle, the battery capacity decreases from 0.386 mAh to 0.316 mAh. During the discharge process, the battery capacity tends to fluctuate from 0.231 to 0.255 mAh and then to 0.241 mAh by the third cycle. While Figure 5f depicts the hematite-based oxalate battery capacity. During the charging procedure, the battery capacity fluctuates between 0.812 and 0.763 mAh, reaching 0.785 mAh during the third cycle. During discharge, the battery capacity stabilizes between 0.636 and 0.633 mAh and approaches 0.625 mAh by the third cycle. According to data on the charge-discharge capacity of batteries with hematite anodes derived from mill scale and oxalate, the stability of battery capacity during the charge and discharge process differs between the two hematite anode varieties. In contrast, batteries containing hematite from oxalate demonstrate greater charge and discharge stability. Despite fluctuations in capacity, fluctuations in value are negligible. The more consistent electrochemical properties of hematite make it possible for the charge-discharge reaction to operate more reliably and with fewer fluctuations in batteries containing hematite as opposed to oxalate [33].

On the basis of Figure 5g about the data of charge efficiency and discharge efficiency for three consecutive cycles, it is evident that fluctuations in efficiency occur for each cycle. The charge efficiency was 59.719% in the first cycle, 70.28 % in the second cycle, and 76.159% in the third cycle. In contrast, the discharge efficiency followed a different pattern, increasing from 78.31% in the first cycle to 83.069% in the second cycle before decreasing to 79.603% in the third cycle. The data indicates that the efficacy of the battery with an oxalate-based hematite anode is marginally greater than on the mill scale. Various factors can cause these fluctuations. During the first cycle, the battery may still be in an unstable initial state, resulting in low charge and discharge efficiencies. Nevertheless, as the cycle progresses, the battery becomes more robust and adapts, resulting in greater charge and discharge efficacy in the second and third cycles. In addition, these fluctuations can be influenced by the impurities of the battery's materials, such as the internal resistance and electrochemical reactions that occur during the charging and discharging processes [34]. In addition to battery cell flaws and environmental factors, fluctuating efficiencies can be caused by imperfect battery cells.

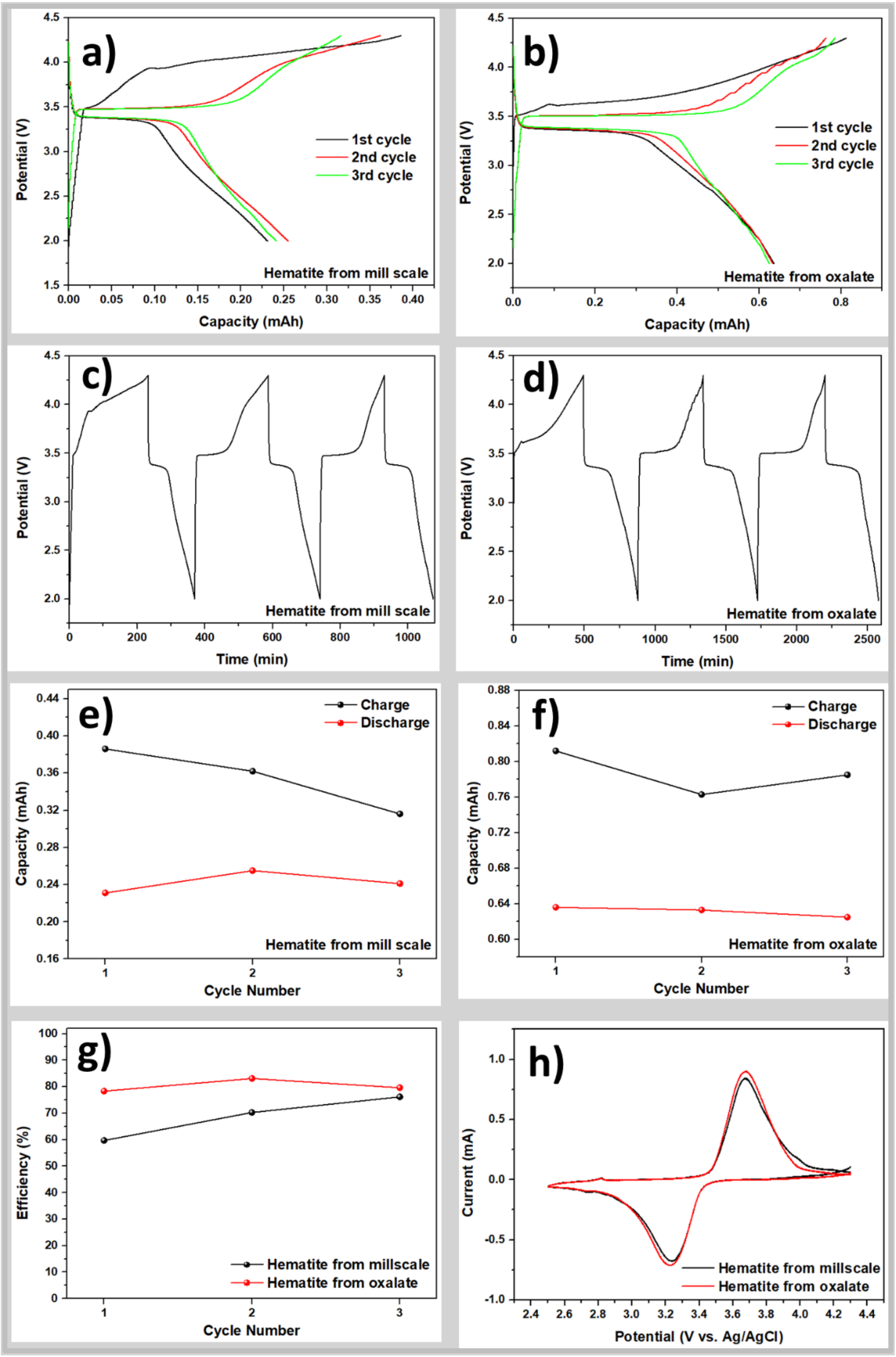

Figure 5. the charge-discharge curve of the battery which uses hematite anode from a) mill scale and b) oxalate as a comparison. While c) and d) is their charge-discharge vs. time curves, e) and f) is their capacity stability curves, g) is efficiency curves and h) is cyclic voltammetry curves

According to the cyclic voltammetry results (Figure 5h), the curve has an oxidation peak at approximately 3.7 V vs. Ag/AgCl and a reduction peak at approximately 3.2 V vs. Ag/AgCl. At the anode (hematite), an oxidation reaction takes place when hematite releases electrons and oxidizes to a higher valence form or loses oxygen. This results in an oxidation peak on the voltammetry curve at approximately 3.7 V versus Ag/AgCl.

Anode (Oxidation): Fe_2O_3 (Hematite) $\rightarrow Fe^{3+} + 3e^-$ (3)

At the cathode (Pt/C), when Pt/C accepts electrons and endures reduction, the reduction reaction occurs. Prior to the cathode's reduction reaction, the anode's (hematite's) oxidation process had previously liberated electrons. This process generates a reduction peak in the voltammetry curve at approximately 3.2 V vs. Ag/AgCl.

Cathode (Reduction): $Pt/C + 3e^- + 3Fe^{3+} \rightarrow Pt + 3Fe^{2+}$ (4)

From Figure 4h, it is clear that the oxidation and reduction peaks of the batteries with hematite anodes made from mill scale and oxalate do not differ by a large margin.

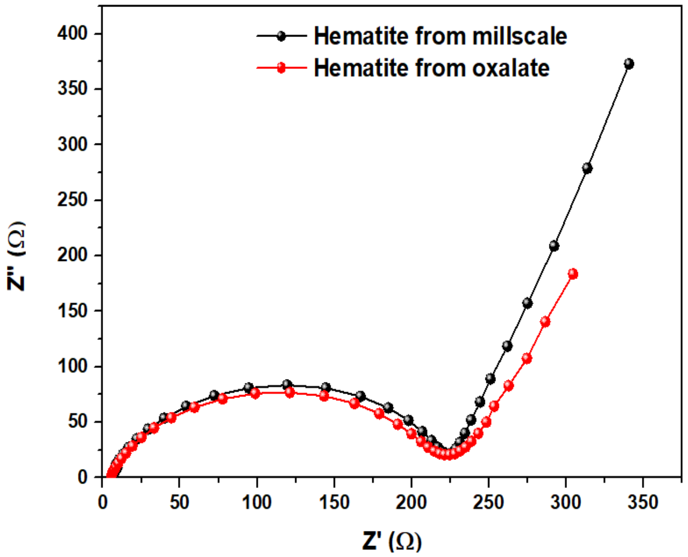

Figure 6. EIS of battery which applies of aluminium foil coated hematite from mill scale and oxalate

On the basis of the electrochemical impedance spectroscopy (EIS) data in Figure 6, two batteries with a hematite anode were investigated, one with an oxalate source and the other with mill scale. The series resistance (R_s) values recorded for both batteries were discovered to be identical at 5.5 Ω. The series resistance is the resistance to current passage through the battery's internal components, such as the electrolyte and electrode interfaces. The similarity in R_s values suggests that both batteries have similar internal resistances, which may contribute to the consistency of their overall performance. However, the charge transfer resistance (R_{ct}) of the two batteries was not significantly different. The Rct value of the hematite anode from oxalate was measured to be 225.2 Ω, while that of the hematite anode from mill scale was 236.5 Ω. R_{ct} represents the resistance associated with charge transfer processes at electrode-electrolyte interfaces [35]. The difference in R_{ct} values between the two anode sources may indicate differences in the kinetics of electron transfer and surface reactions.

4. CONCLUSION

This study investigated the effects of varying the amount of $CaCO_3$ pellets and calcination time on the purity of hematite produced and the impact of deposition time and voltage on coating thickness. The findings suggest that an increase in calcination time results in a higher purity percentage of hematite while increasing the number of $CaCO_3$ pellets decreases slightly on the purity of the resulting hematite. The ideal amount of $CaCO_3$ pellets required should be used to ensure that the reaction is successful and that the resultant hematite is of high purity. Other variables such as temperature, time, and electrolyte concentrations may also influence the purity of the resultant hematite and should be considered concurrently to achieve an ideal output. In the case of deposition time and voltage, the findings indicate that there is a saturation threshold of the coating thickness beyond which the thickness drops. The thickest layer was achieved with a 40 V treatment and a deposition duration of 30 minutes. This suggests that the voltage treatment and deposition duration have a selective effect on the particle size and thickness of the resultant layer. Overall, the study provides insight into the factors that affect the quality of hematite and the thickness of the coating on the surface of an electrode. batteries with hematite anodes derived from oxalate exhibit superior performance compared to those derived from mill scale, demonstrated by higher charge capacity, discharge capacity, and charge-discharge cycle time. The crystal structure and homogeneity of hematite from oxalate contribute to more efficient charge transfer during the charge-discharge process. Additionally, the batteries containing hematite from oxalate demonstrate greater stability in charge and discharge capacities, indicating their potential for enhanced energy storage applications. Further research could explore the other factors that may affect the quality of hematite and the coating thickness, such as the type of $CaCO_3$ pellets used and the composition of the electrode surface. Overall, the study contributes to the development of more efficient and effective production processes for hematite and its applications in battery anode.

Acknowledgements

This project was partially supported by the Hibah Program Kompetisi Kampus Merdeka (PKKM) of being funded by the Indonesian Ministry of Education, Culture, Research and Technology, with contract number: 65/E1/KM.05.03/2021. The authors also acknowledge the facilities, scientific, and technical support from Advanced Characterization Laboratories Serpong, National Research and Innovation Agency through E-Layanan Sains (ELSA), the Badan Riset and Inovasi National (BRIN).

Declarations of interest

The authors declare no conflict of interest in this reported work.

REFERENCES

[1] D.A. Iluțiu-Varvara, M. Tintelecan, C. Aciu, and I.M. Sas-Boca, Multidisciplinary Digital Publishing Institute Proceedings 63 (2020) 14.

[2] J. Shen, R. Gonçalves, Y.T. Choi, J.G. Lopes, J. Yang, N. Schell, and J. P. Oliveira, Scr. Mater. 222 (2023) 115053.

[3] J. Shen, R. Gonçalves, Y.T. Choi, J.G. Lopes, J. Yang, N. Schell, and J. P. Oliveira, Mater. Sci. Eng. A 857 (2022) 144025.

[4] J. Shen, P. Agrawal, T.A. Rodrigues, J.G. Lopes, N. Schell, Z. Zeng, and J. P. Oliveira, Mater. Des. 223 (2022) 111176.

[5] J. Shen, P. Agrawal, T.A. Rodrigues, J.G. Lopes, N. Schell, J. He, and J. P. Oliveira, Mater. Sci. Eng. A 867 (2023) 144722.

[6] F. Nurjaman, N.M. Prilitasari, A.E. Prasetyo, and E. Nugroho, Metallurgy 34 (2019) 37.

[7] D. Nayak, S.K. Roy, N. Dash, and S.S. Rath, Trans. Indian Inst. Met. 73 (2020) 691.

[8] D.S. Khaerudini, I. Chanif, D.R. Insiyanda, F. Destyorini, S. Alva, and A. Pramono, J. Sustain. Metall. 5 (2019) 510.

[9] M.T., Aldiramadan, J., Nabilah, M., Ridwan, and D.S. Khaerudini, IOP Conf. Ser.: Mater. Sci. Eng. 1195 (2021) 012044.

[10] W. Annisa, I. N. Manyoe, A.K. Mubarak, S. S. S. Napu, I.G.S. Pratama, and S. Fatimah, IOP Conf. Ser.: Earth Environ. Sci. 589 (2020) 012021

[11] M.S. Quddus, M. Rahman, J. Khanam, B. Biswas, N. Sharmin, S. Ahmed, and A. Neger, Int. Res. J. Pure Appl. Chem. 16 (2018) 1.

[12] D.S. Khaerudini, W. Yulistia, I. Royani, D.R. Insiyanda, and S. Alva, J. Sustain. Metall. 55 (2020) 192.

[13] W.R.W. Ahmad, M.H. Mamat, A.S. Zoolfakar, Z. Khusaimi, and M. Rusop, IEEE Student Conference on Research and Development (SCOReD) (2016) 1.

[14] L. Besra, and M. Liu, Progress in Materials Science 52 (2007) 1.

[15] A. Rafique, I. Sequeira, A.S. Bento, M.P. Moniz, J. Carmo, E. Oliveira, and A.C. Baptista, Chem. Eng. J. 464 (2023) 142515.

[16] S. Vaez, R. Emadi, S. Sadeghzade, H. Salimijazi, and M. Kharaziha, Mater. Chem. Phys. 282 (2022) 125991.

[17] S. Zeng, K. Tang, T. Li, Z. Liang, D. Wang, Y. Wang, and W. Zhou, J. Phys. Chem. C 112 (2008) 4836.

[18] B. M. Klahr, and T. W. Hamann, J. Phys. Chem. C 115 (2011) 8393.

[19] P. Biswas, A. Ainabayev, A. Zhussupbekova, F. Jose, R. O’Connor, A. Kaisha, and I.V. Shvets, Sci. Rep. 10 (2020) 7463.

[20] P.C. Jikar, R. Sabban, C. Tadwalkar, and N.B. Dhokey, Mater. Today 44 (2021) 4013.

[21] L. Niu, Z. Liu, J. Zhang, D. Lan, S. Li, Z. Li, and Y. Wang, Int. J. Miner. Metall. Mater. 30 (2023) 303.

[22] Z. Zhang, Q. Yang, and S. Wu, IEEE Trans. Dielectr. Electr. Insul. 28 (2021) 600.

[23] X. Chen, M. Wang, J. Chen, and S. Shen, J. Mater. Res. 31 (2016) 1547.

[24] B. L. Bennett, E. C. Wyatt, and C. T. Harris, Ind. Eng. Chem. Res. 55 (2016) 11583.

[25] B. M. Klahr, and T. W. Hamann, J. Phys. Chem. C 115 (2011) 8393.

[26] S.M. Sharif, N.F.A. Bakar, and M.N. Naim, J. Water Process. Eng. 7 (2015) 123.

[27] S.S. Shinde, R.A. Bansode, C.H. Bhosale, and K.Y. Rajpure, J. Semicond. 32 (2011) 013001.

[28] L.P.H. Jeurgens, W.G. Sloof, F.D. Tichelaar, and E. J. Mittemeijer, Thin Solid Films. 418 (2002) 89.

[29] C. Liu, Y. Chen, S. Song, and H. Li, Colloids Surf. A: Physicochem. Eng. 555 (2018) 708.

[30] D.A. Almasri, N.B. Saleh, M.A. Atieh, G. McKay, and S. Ahzi, Sci. Rep. 9 (2019) 3232.

[31] A. Mitsuo, S. Uchida, N. Nihira, and M. Iwaki, Surf. Coat. Technol. 103 (1998) 98.

[32] X. Dong, Y. Yang, B. Wang, Y. Cao, N. Wang, P. Li, and Y. Xia, Adv. Sci. 7 (2020) 2000196.

[33] H. Huang, L. Kong, J. He, M. Liu, J. Zhang, and X.H. Bu, J. Solid State Chem. 305 (2022) 122639.

[34] M. Pahlevaninezhad, M. Pahlevani, and E.P. Roberts, J. Power Sources 529 (2022) 231271.

[35] M. Christwardana, Y. Chung, and Y. Kwon, Korean J. Chem. Eng. 34 (2017) 3009.